



HAL
open science

Effects of climate change and seed dispersal on airborne ragweed pollen loads in Europe

Lynda Hamaoui-Laguel, Robert Vautard, Li Liu, Fabien Solmon, Nicolas N. Viovy, Dmitry Khvorostyanov, Franz Essl, Isabelle Chuine, Augustin Colette, Mikhail A. Semenov, et al.

► To cite this version:

Lynda Hamaoui-Laguel, Robert Vautard, Li Liu, Fabien Solmon, Nicolas N. Viovy, et al.. Effects of climate change and seed dispersal on airborne ragweed pollen loads in Europe. *Nature Climate Change*, 2015, 5 (8), pp.766-771. 10.1038/NCLIMATE2652 . hal-01806139

HAL Id: hal-01806139

<https://hal.science/hal-01806139v1>

Submitted on 22 Sep 2022

HAL is a multi-disciplinary open access archive for the deposit and dissemination of scientific research documents, whether they are published or not. The documents may come from teaching and research institutions in France or abroad, or from public or private research centers.

L'archive ouverte pluridisciplinaire **HAL**, est destinée au dépôt et à la diffusion de documents scientifiques de niveau recherche, publiés ou non, émanant des établissements d'enseignement et de recherche français ou étrangers, des laboratoires publics ou privés.



Distributed under a Creative Commons Attribution 4.0 International License

Effects of climate change and seed dispersal on airborne ragweed pollen loads in Europe

Lynda Hamaoui-Laguel^{1,2*}, Robert Vautard^{1*}, Li Liu³, Fabien Solmon³, Nicolas Viovy¹, Dmitry Khvorostyanov⁴, Franz Essl⁵, Isabelle Chuine⁶, Augustin Colette², Mikhail A. Semenov⁷, Alice Schaffhauser¹, Jonathan Storkey⁷, Michel Thibaudon⁸ and Michelle M. Epstein⁹

¹Laboratoire des Sciences du Climat et de l'Environnement, IPSL, CEA-CNRS-UVSQ, UMR8212, 91191 Gif sur Yvette, France

²Institut National de l'Environnement Industriel et des Risques, Parc technologique ALATA, 60550 Verneuil en Halatte, France

³Earth System Physics Section, International Centre for Theoretical Physics, 34100 Trieste, Italy

⁴Laboratoire de Météorologie Dynamique, IPSL, CNRS, UMR8539, 91120 Palaiseau, France

⁵Division of Conservation Biology, Vegetation and Landscape Ecology, Faculty Centre of Biodiversity, University of Vienna, 1030 Vienna, Austria

⁶CEFE UMR 5175, CNRS - Université de Montpellier—1919 route de Mende, 34293 Montpellier cedex 05, France

⁷Rothamsted Research, Harpenden, Hertfordshire AL5 2JQ, UK

⁸Réseau National de Surveillance Aérobiologique, 69690 Brussieu, France

⁹Department of Dermatology, Division of Immunology, Allergy and Infectious Diseases, Experimental Allergy, Medical University of Vienna, 1090 Vienna, Austria.

Common ragweed (Ambrosia artemisiifolia) is an invasive alien species in Europe producing pollen that causes severe allergic disease in susceptible individuals¹. Ragweed plants could further invade European land with climate and land-use changes^{2,3}. However, airborne pollen evolution depends not only on plant invasion, but also on pollen production, release and atmospheric dispersion changes. To predict the effect of climate and land-use changes on airborne pollen concentrations, we used two comprehensive modelling frameworks accounting for all these factors under high-end and moderate climate and land-use change scenarios. We estimate that by 2050 airborne ragweed pollen concentrations will be about 4 times higher than they are now, with a range of uncertainty from 2 to 12 largely depending on the seed dispersal rate assumptions. About a third of the airborne pollen increase is due to on-going seed dispersal, irrespective of climate change. The remaining two-thirds are related to climate and land-use changes that will extend ragweed habitat suitability in northern and eastern Europe and increase pollen production in established ragweed areas owing to increasing CO₂. Therefore, climate change and ragweed seed dispersal in current and future suitable areas will increase airborne pollen concentrations, which may consequently heighten the incidence and prevalence of ragweed allergy.

Common ragweed is native in North America. Since the end of the nineteenth century it has invaded large regions in Europe^{4,5} and also parts of Australia, South America and East Asia⁶. The sensitization of the human population to ragweed pollen is increasing in many countries⁷. In Europe, its established presence is at present largely limited to several areas in the [42° N–47° N] latitudinal band (Pannonian plain, northern Italy and southeastern France) and in areas with disturbed land, such as agricultural areas or along roads and railways. However, there is a high potential for further spread given that suitable, although not yet invaded, habitats are substantial^{8,9}. Plant density may also further increase in established infested areas. Factors determining the rate of spread of ragweed plants within its current climatic niche include seed dispersal due to natural or anthropogenic processes (for example, spread through contaminated crop seeds), land-use change (which

would provide changes in disturbed land areas) and the efficiency of ragweed eradication policies. Climate change may further impact the spread of ragweed by altering the climatic niche determined by physiological thresholds or affecting cropping patterns^{5,10,11}. Ragweed airborne pollen concentrations depend not only on plant infestation, but also on phenology, pollen production, release, dispersion and atmospheric transport. Recent modelling efforts^{12–15} have led to increasingly successful simulations of airborne pollen concentrations. Although previous work was mostly devoted to short-term forecasts to inform sensitized populations, the maturity of the modelling tools are now becoming satisfactory for engaging in long-term projections.

Here, we present the first integrated modelling framework that incorporates ragweed phenology, pollen production, release and atmospheric transport to assess future changes in airborne pollen concentration under scenarios of climate and land-use changes and seed dispersal. The framework is based on an explicit representation of plant phenology¹⁶, pollen production¹⁷, and release to the atmosphere¹² (see Methods and Supplementary Information). We implemented two model suites that differ in the atmospheric processing and in the driving climate models. The first model uses the chemistry-transport model (CTM) CHIMERE model¹⁸, forced by recent regional climate simulations from the WRF model¹⁹ downscaling of the IPSL-CM5A-MR model²⁰. The other model uses the RegCM4 regional climate model with online chemistry and transport²¹ forced by global climate simulations from HadGEM CMIP5 (ref. 22). In both modelling set-ups, the same 50 km grid was used over Europe. Hereafter, the two suites will be respectively called CHIMERE and RegCM for the sake of simplicity. The reference historical period is 1986–2005 and the future period considered is 2041–2060. We selected two contrasting RCPs (Representative Concentration Pathways) climate change scenarios²³, including a high-end (RCP 8.5) and a moderate (RCP 4.5) climate change scenario.

The current ragweed density distribution at a 50 km resolution was calculated using a dataset taken from a previous study⁵, which reported the presence of ragweed plants for a grid of 10 × 10 km based on the plant observations, combined with a climate habitat suitability index computed by a weather-driven,

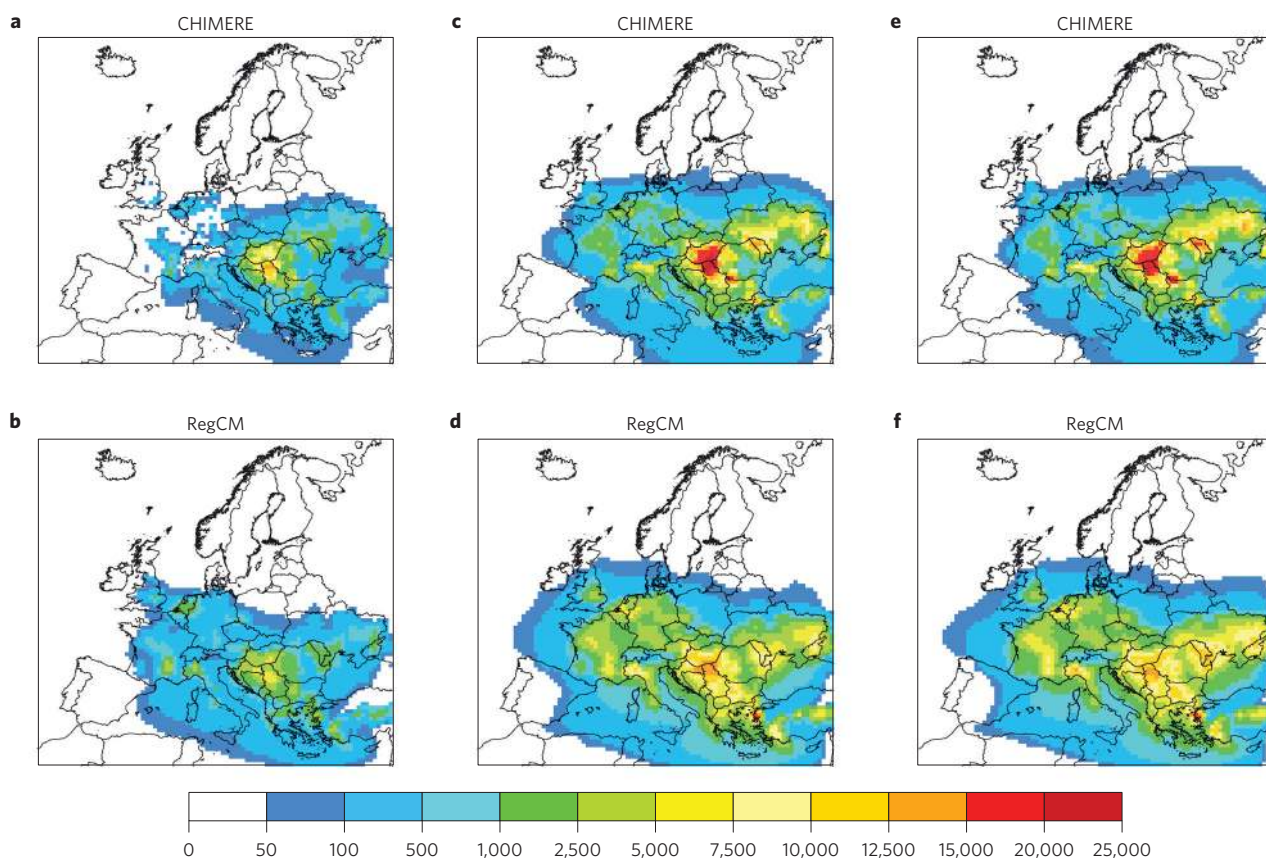


Figure 1 - Simulated historical and future average annual ragweed pollen counts in grains m⁻³. a,b, Historical average pollen counts (1986–2005). c–f, Evolution of annual pollen counts in 2050 under moderate (RCP 4.5, c,d) and high-end (RCP 8.5, e,f) climate change scenarios.

process-based model of ragweed growth and development³ including the plant phenology and change in season length due to later frosts, and the fractional area of suitable habitats for ragweed (crops and urban lands). Given the high uncertainty of ragweed distribution, a calibration procedure was applied using observed mean airborne pollen counts over Europe (see Methods and Supplementary Information). A simplified seed dispersal model was used to project ragweed density distribution in 2050, extending a previous model applied for central Europe¹¹ (see Methods and Supplementary Information).

The two models reproduced the observed mean daily pollen counts and their spatial distribution well when using ERA-Interim re-analyses weather forcing—with Pearson correlations of 0.77 with CHIMERE and 0.95 with RegCM (Supplementary Fig. 1). This is partly due to the calibration methodology, but cross-validation experiments with calibration for subsets of stations and verification for complementary subsets showed the robustness of the approach for the spatial pollen count distribution (Supplementary Fig. 1). Using global circulation model (GCM) forcing instead of re-analyses forcing did not greatly alter the simulated pollen counts (Supplementary Fig. 2).

For the mid twenty-first century, the two models projected increasing pollen concentrations for large regions of Europe, regardless of the climate scenario (Fig. 1). Pollen loads become substantial in areas where they are at present virtually zero (north-central Europe, northern France and southern UK). In current high pollen level areas (for example, the Pannonian plain), concentrations increase up to an approximate factor of two. On average, annual pollen loads are projected to increase by a factor of 4.5 under high-end (RCP 8.5) and 4.0 under moderate (RCP 4.5) climate change scenarios. The relative increase is higher in northern

Europe because current loads are small and any increase will be significant, whereas in south/central Europe current loads are high. However, in absolute numbers, the increase in the latter areas can be larger, which represents higher risk for the population.

Alternative sensitivity simulations were carried out to assess the relative contributions of the different drivers: excluding seed dispersal to quantify the direct effect of climate change on pollen production by already established populations; excluding climate change to quantify the effect of seed dispersal filling in the available climate niche under current climate conditions; and limiting the effect of climate change to its impact on ragweed distribution, excluding the impact on plant pollen production, release and dispersion. The expansion of regions with high annual pollen concentrations is primarily driven by ragweed spread (Supplementary Fig. 3), owing to the combined effects of increased habitat suitability induced by climate and land-use changes, and to seed dispersal over time. Without dispersal, changes in climate would lead to an increase reaching on average only 13% and 17% (for resp. CHIMERE and RegCM) of the increase with all processes.

In contrast, seed dispersal by 2050, in the absence of climate change, contributes to about a third of the average increase in pollen loads in Europe (44% for CHIMERE and 29% for RegCM) and much higher values in northwestern Europe³ (Fig. 2c,d). The impact of climate change on plant habitat suitability will exacerbate the projected invasion, especially in eastern Europe (Fig. 2e,f), from Croatia and Hungary towards the whole Balkan region and Ukraine (Supplementary Fig. 3c,d). However, caution should be taken concerning spread in Ukraine because the current ragweed distribution is poorly documented⁵. The expansion of the ragweed plant distribution due to the combination of seed dispersal and climate change on habitat suitability will contribute 43% (with

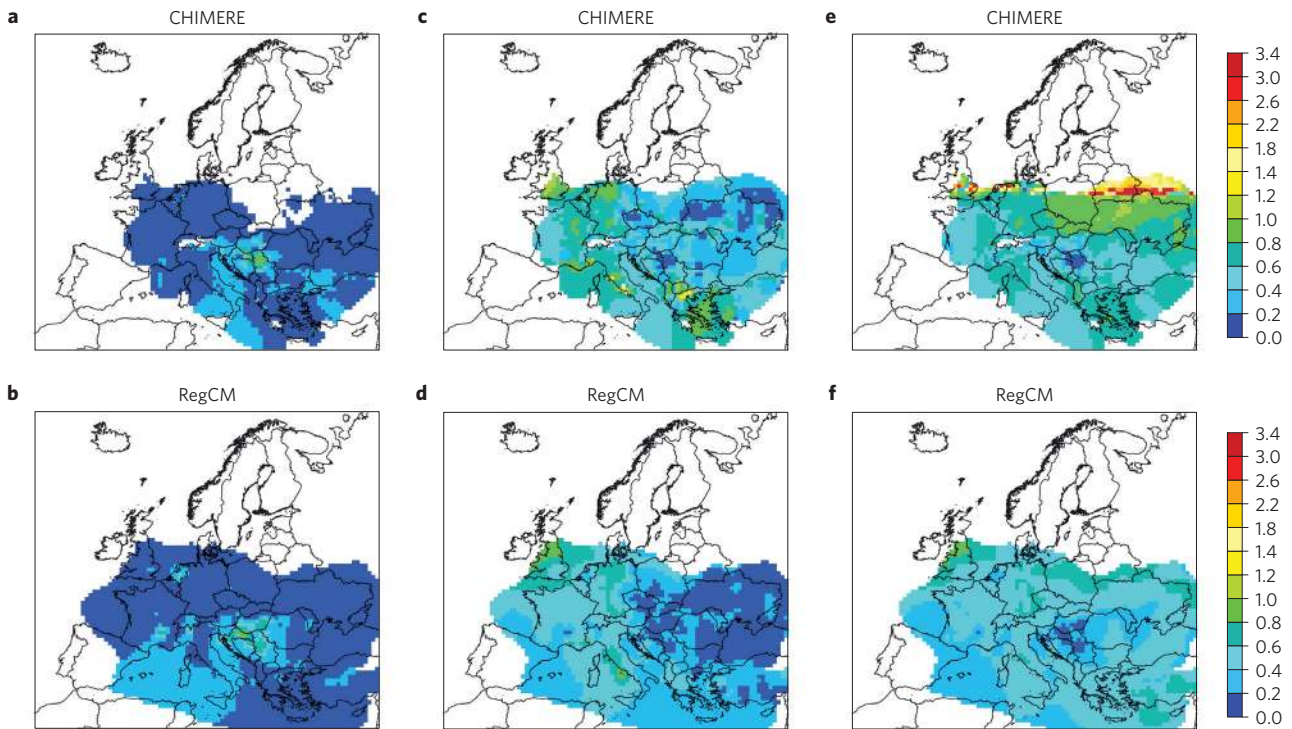


Figure 2 - Contributions to pollen count change relative to historical pollens between test and reference simulations for 2050 (RCP 8.5). a,b, Without seed dispersal but considering the impact of climate change on pollen production, release and transport. c,d, With seed dispersal until 2050 but without effects of climate change. e,f, With seed dispersal and impact of climate change on habitat suitability only. Contributions are calculated as ratios to the change in the reference future simulation including seed dispersal scenario and impact of climate change on habitat suitability, pollen production and release, as in Fig. 1e-f.

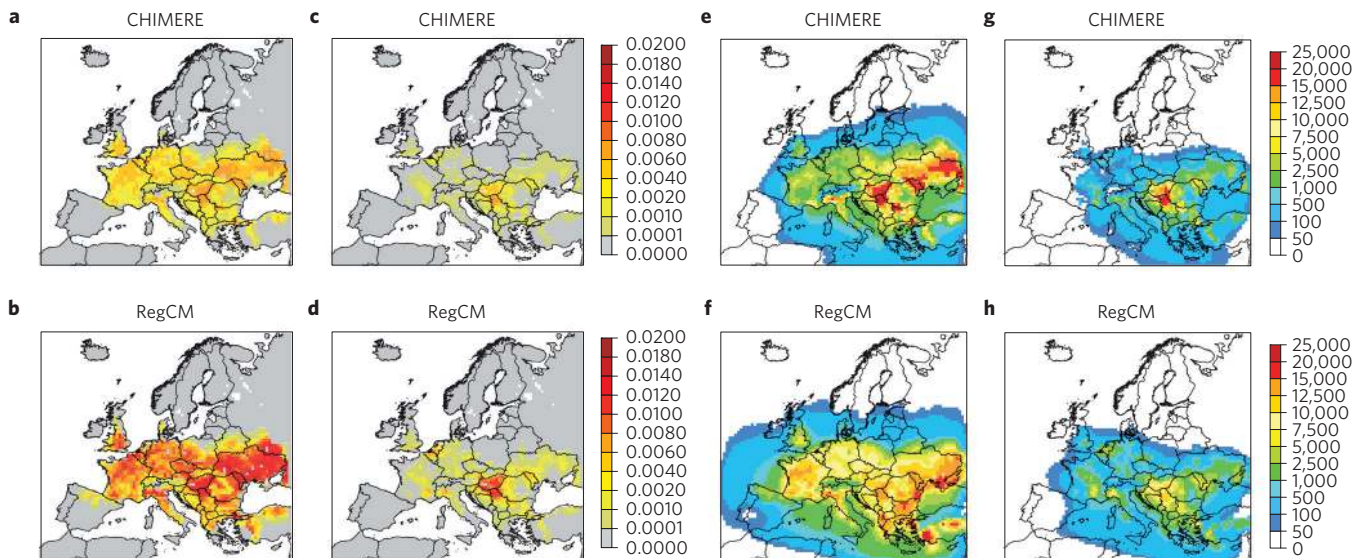


Figure 3 - Impact of rapid and slow seed dispersal scenarios on simulated ragweed distribution and airborne pollen counts for 2050 (RCP 8.5). a-d, Ragweed distribution density (plants m^{-2}) considering rapid I2 (a,b) and slow I3 (c,d) scenarios. e-h, Projected annual airborne pollen counts (grains m^{-3}) considering rapid I2 (e,f) and slow I3 (g,h) ragweed spread scenarios.

RegCM) and 70% (with CHIMERE) of the mean European airborne pollen change. The remaining contribution (30% for CHIMERE and 57% for RegCM) is attributed to changes in pollen production, release and dispersion, from this expanded distribution.

Spread rates of alien species are subject to uncertainties, not only due to habitat suitability change, but also to the modes and rate of seed dispersal. The simplified reference dispersal process

used (I1) assumes that fluxes of seeds from one place to another are inversely proportional to the square of their distance, as in previous studies¹¹. For uncertainty estimations, we changed the proportionality coefficient according to ranges previously estimated for central Europe¹¹ to analyse rapid (I2, Fig. 3a,b) and slow (I3, Fig. 3c,d) seed dispersal scenarios for 2050. The differences between distributions obtained with the two climate scenarios (see

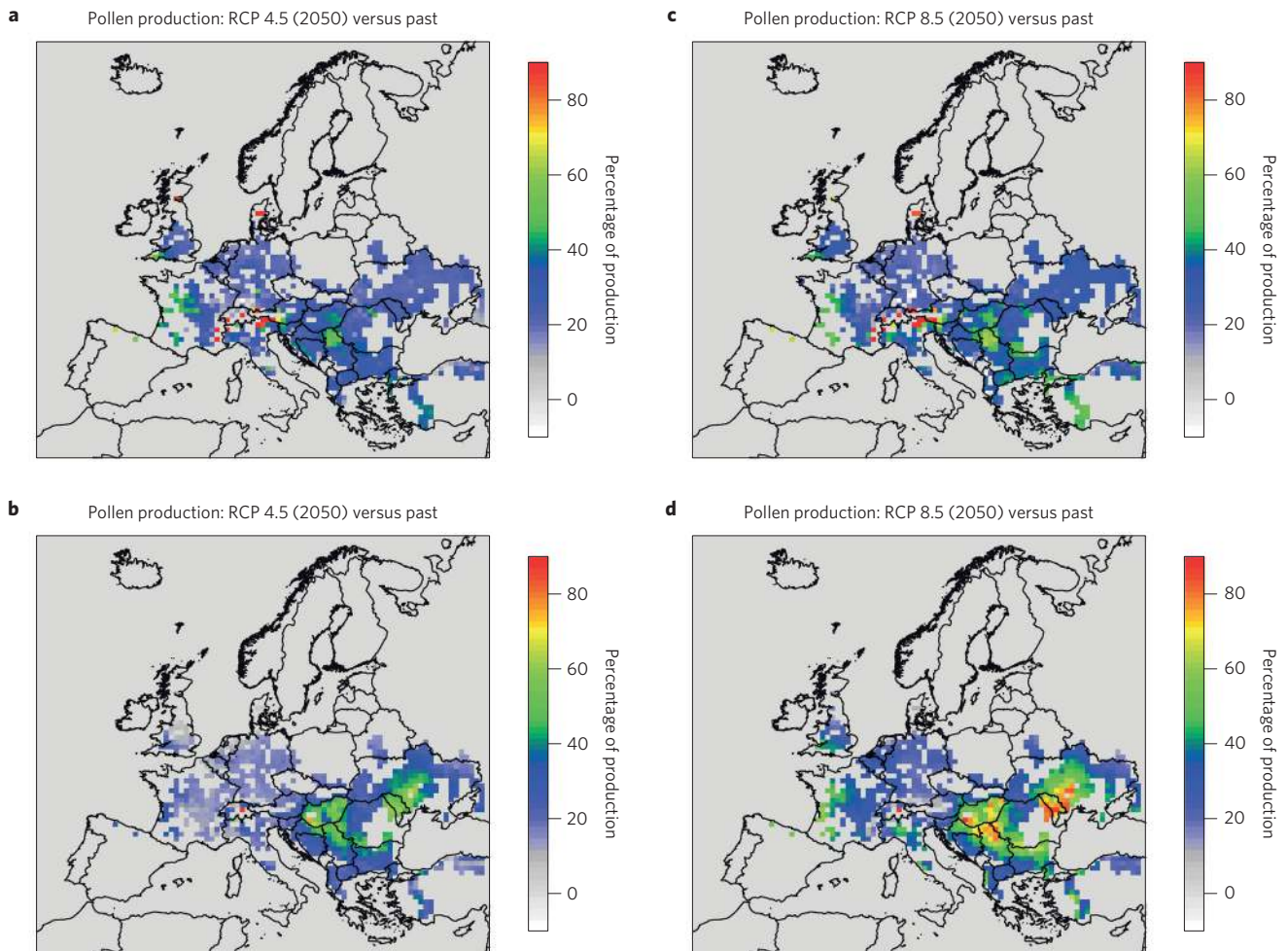


Figure 4 - Evolution of average pollen production (in percent) in 2050. a,b, Under a moderate (RCP 4.5) climate change scenario. c,d, Under a high (RCP 8.5) climate change scenario. Historical (1986–2005) and future simulations (2041–2060) are calculated by ORCHIDEE with IPSL-CM5A-MR/WRF (a,c) and HadGEM-CMIP5/RegCM (b,d) meteorological data, considering the historical ragweed distribution density.

Supplementary Fig. 3e,f) are smaller than the differences between distributions obtained with fast and slow dispersal rates. Depending on the rate of seed dispersal, the resulting projections of ragweed density in 2050 for Europe (mean of the two suites of models) vary on average by a factor of 6.1 under high-end (RCP 8.5) and 5.6 under moderate (RCP 4.5) climate change.

This large uncertainty is due to ragweed spread that is limited by dispersal rates, and at present incomplete range infilling due to a lagged colonization of suitable habitats. As a result, simulated airborne pollen counts differ substantially, depending on the choice of dispersal rates (Fig. 3e–h), for both modelling suites. Under rapid seed dispersal, in 2050, the pollen concentrations are projected to become as large as or exceed current counts in Hungary in parts of eastern Europe (Ukraine) and Russia. In France, Germany and southern UK, concentrations largely increase and will exceed values at present observed in the south of France. Under slow seed dispersal, pollen patterns are primarily driven by the direct impact of climate change on production and transport rather than on range expansion of ragweed. Hence, the results are close to those using the current distribution (Supplementary Fig. 4).

Importantly, even under climate scenario RCP 8.5 and rapid spread, high pollen concentrations remain bounded within central and eastern Europe. High total annual counts (up to 22,000 grains m^{-3}) are found in the Balkans, Ukraine and northern Italy. In France, Germany and southern UK, average total counts range for the reference and rapid spread scenarios, respectively,

in the 460–3,700 and 1,800–8,000 grains m^{-3} for CHIMERE and 1,800–7,400 and 3,700–12,900 grains m^{-3} for RegCM. In the rapid seed dispersal scenario, concentrations obtained with RegCM in parts of France will reach the same values as in the highly-infested areas in central and eastern Europe, whereas with CHIMERE we found a clear difference between western and eastern parts of Europe.

We conclude that the rate of seed dispersal will have a key influence on future pollen loads. However, even in the absence of any change in ragweed distribution, climate change will induce an increase in pollen loads (Fig. 2a,b). For instance, high pollen counts are projected in regions where current levels are estimated to be relatively weak (for example, central France) and the absolute increase can reach 4,000–7,500 grains m^{-3} in central and eastern Europe (for example, Hungary and Serbia). These changes are possibly caused by enhanced pollen production and climatic conditions more favourable to release and airborne pollen accumulation (typically dry anticyclonic period with weak winds).

Pollen production increases, owing to the enhanced photosynthetic rate and biomass at higher CO_2 levels²⁴, even if large uncertainties remain on the scale of the actual CO_2 fertilization effect, as it is constrained under field conditions, for example, by nitrogen availability²⁵. The extension of the growing season length in temperate regions²⁶ also increases pollen production. These effects could be partly offset by a decrease of precipitation during the growth period, causing water stress and a

decrease of net primary production. In our simulations (without seed dispersal), future pollen production in 2050 calculated by the vegetation model, using current ragweed distribution, are higher than the historical production by 29–31% under moderate (RCP 4.5) and 36–43% under high-end (RCP 8.5) climate change scenarios using CHIMERE and RegCM model suites, respectively (Fig. 4). The effect of climate change on ragweed phenology and season length helps extending habitat suitability³ in the northern limit of Europe. However, the effect of climate change on pollen production through the start and the end of pollen season²⁶ for a fixed ragweed distribution is less important than the CO₂ effect. In the CHIMERE suite, our results (not shown) indicate that in 2050 the end of the season is delayed by a few days compared to historical climate, and the pollen season starts one to ten days earlier because of accelerated ragweed development with higher temperatures.

Nevertheless, the models do not at present account for the potential of populations at the edge of the range to adapt to new conditions, which may both extend the range of suitable habitat for ragweed and the period of pollen production.

The pollen production increase dominates over release and dispersion changes in explaining the differences between future and historical climate airborne pollen concentrations (Supplementary Fig. 5a). Moreover, increased CO₂ concentrations are the main driving factor for pollen production increase (Supplementary Fig. 5b).

Our simulations demonstrate that future ragweed airborne pollen loads are likely to increase in large parts of Europe owing to the synergistic effects of climate change on habitat suitability, pollen production, release and transport, and the infilling of existing suitable habitats due to seed dispersal. We estimated that seed dispersal accounts for about a third of the future airborne pollen increase irrespective of climate change, whereas climate change explains the other two-thirds. As well as the predicted increase in airborne pollen loads, the allergenicity of ragweed pollens may increase under expected global changes²⁷. Therefore, any future allergies linked to ragweed pollens would be exacerbated.

Once established, ragweed is difficult to eradicate because of its long-lived seed, its capacity to re-sprout after cutting and its propensity to evolve resistance to herbicides²⁸. Our results indicate that controlling the current European ragweed invasion will become more difficult in the future as the environment will be more favourable for ragweed growth and spread, highlighting the need for the development of effective and regionally co-ordinated eradication programmes. The high sensitivity to seed dispersal and the fact that long-distance dispersal of ragweed is driven by human activity⁵ also emphasize the importance of measures to control the spread of contaminated crop seed and monitor regions prone to new invasions.

References

- Kazinczi, G., Beres, I., Pathy, Z. & Novak, R. Common ragweed (*Ambrosia artemisiifolia* L.): A review with special regards to the results in Hungary: II. Importance and harmful effect, allergy, habitat, allelopathy and beneficial characteristics. *Herbologia* **9**, 93–118 (2008).
- Essl, F. *et al.* Biological Flora of the British Isles: *Ambrosia artemisiifolia*. *J. Ecol.* (in the press).
- Storkey, J., Stratonovitch, P., Chapman, D. S., Vidotto, F. & Semenov, M. A. A process-based approach to predicting the effect of climate change on the distribution of an invasive allergenic plant in Europe. *PLoS ONE* **9**, e88156 (2014).
- Chauvel, B., Dessaint, F., Cardinal-Legrand, C. & Bretagnolle, F. The historical spread of *Ambrosia artemisiifolia* L. in France from herbarium records. *J. Biogeogr.* **33**, 665–673 (2006).
- Bullock, J. *et al.* *Assessing and Controlling the Spread and the Effects of Common Ragweed in Europe* Report No. ENV.B2/ETU/2010/0037 (EU Commission, 2012).
- Scalera, R., Genovesi, P., Essl, F. & Rabitsch, W. *The Impacts of Invasive Alien Species in Europe* Report No. 16 (EEA, 2012).

- Burbach, G. J. *et al.* Ragweed sensitization in Europe – GA2LEN study suggests increasing prevalence. *Allergy* **64**, 664–665 (2009).
- Vogl, G. *et al.* Modelling the spread of ragweed: Effects of habitat, climate change and diffusion. *Eur. Phys. J. Spec. Top.* **161**, 167–173 (2008).
- Smolik, M. G. *et al.* Integrating species distribution models and interacting particle systems to predict the spread of an invasive alien plant. *J. Biogeogr.* **37**, 411–422 (2010).
- Cunze, S., Leiblein, M. C. & Tackenberg, O. Range expansion of *Ambrosia artemisiifolia* in Europe is promoted by climate change. *ISRN Ecol.* **2013**, 610126 (2013).
- Richter, R., Dullinger, S., Essl, F., Leitner, M. & Vogl, M. How to account for habitat suitability in weed management programmes? *Biol. Invasions* **15**, 657–669 (2013).
- Efstathiou, C., Isukapalli, S. & Georgopoulos, P. A mechanistic modeling system for estimating large scale emissions and transport of pollen and co-allergens. *Atmos. Environ.* **45**, 2260–2276 (2011).
- Zink, K., Vogel, H., Vogel, B., Magyar, D. & Kottmeier, C. Modeling the dispersion of *Ambrosia artemisiifolia* L. pollen with the model system COSMO-ART. *Int. J. Biometeorol.* **56**, 669–680 (2012).
- Prank, M. *et al.* An operational model for forecasting ragweed pollen release and dispersion in Europe. *Agric. For. Meteorol.* **182–183**, 43–53 (2014).
- Chapman, D. S., Haynes, D., Beal, S., Essl, F. & Bullock, J. Phenology predicts the native and invasive range limits of common ragweed. *Glob. Change Biol.* **20**, 192–202 (2014).
- Chuine, I., Garcia de Cortazar Atauri, I., Kramer, K. & Hänninen, H. in *Phenology: An Integrative Environmental Science* (ed. Schwarz, M. D.) 275–293 (Springer, 2013).
- Krinner, G. *et al.* A dynamic global vegetation model for studies of the coupled atmosphere-biosphere system. *Glob. Biogeochem. Cycle* **19**, GB1015 (2005).
- Menut, L. *et al.* CHIMERE 2013: A model for regional atmospheric composition modelling. *Geosci. Model Dev.* **6**, 981–1028 (2013).
- Vautard, R. *et al.* The simulation of European heat waves from an ensemble of regional climate models within the EURO-CORDEX project. *Clim. Dynam.* **41**, 2555–2575 (2013).
- Dufresne, J.-L. *et al.* Climate change projections using the IPSL-CM5 Earth System Model: From CMIP3 to CMIP5. *Clim. Dynam.* **40**, 2123–2165 (2013).
- Giorgi, F. *et al.* RegCM4: Model description and preliminary tests over multiple CORDEX domains. *Clim. Res.* **52**, 7–29 (2012).
- Collins, W. J. *et al.* Development and evaluation of an Earth-System model-HadGEM2. *Geosci. Model Dev.* **4**, 1051–1075 (2011).
- Moss, R. H. *et al.* The next generation of scenarios for climate change research and assessment. *Nature* **463**, 747–756 (2010).
- Ziska, L. H. & Caulfield, F. A. Rising CO₂ and pollen production of common ragweed (*Ambrosia artemisiifolia*), a known allergy-inducing species: Implications for public health. *Aust. J. Plant Physiol.* **27**, 893–898 (2000).
- Reich, P. B. *et al.* Nitrogen limitation constrains sustainability of ecosystem response to CO₂. *Nature* **440**, 922–925 (2006).
- Ziska, L. H. *et al.* Recent warming by latitude associated with increased length of ragweed pollen season in central North America. *Proc. Natl Acad. Sci. USA* **108**, 4248–4251 (2011).
- El Kelish, A. *et al.* Ragweed (*Ambrosia artemisiifolia*) pollen allergenicity: SuperSAGE transcriptomic analysis upon elevated CO₂ and drought stress. *BMC Plant Biol.* **14**, 176 (2014).
- Brewer, C. E. & Oliver, L. R. Confirmation and resistance mechanisms in glyphosate-resistant common ragweed (*Ambrosia artemisiifolia*) in Arkansas. *Weed Sci.* **57**, 567–573 (2009).

Acknowledgements

This study was carried out within the ‘Atopic diseases in changing climate, land use and air quality’ (ATOPICA) FP7 Project, under grant agreement #282687. We are grateful to all pollen data providers from the European Aeroallergen Network (<https://ean.polleninfo.eu>), the French aerobiology network RNSA (<http://www.pollens.fr>), ARPA-Veneto and ARPA-FVG (Italy). We are also grateful to A. Cvitković and N. Periš from the Croatian Institute of Public Health (counties of Brodsko-Posavska and Splitsko-Dalmatinska, respectively), B. Stjepanović from the Department of Environmental Protection and Health Ecology Institute of Public Health ‘Andrija Stampar’ (Zagreb) and R. Peternel from the Associate-degree college of Velika Gorica, for providing pollen measurements. We thank J.-P. Besancenot for critical reading of the manuscript.

Author contributions

L.H.-L. led the study, designed and conducted the CHIMERE experiments. L.L. and F.S. developed and conducted the parallel experiments with RegCM. D.K. developed the pollen version of CHIMERE, and N.V. developed the pollen production module in ORCHIDEE. R.V. coordinated the pollen modelling ATOPICA work package (WP2) and M.M.E. coordinated the ATOPICA project. J.S. and M.A.S. provided the methodology and climate habitat suitability results. I.C. provided the PMP phenology model and contributed to the development of the ragweed phenological model. F.E. provided advice and helped in designing the experiments. M.T. provided the French monitoring data and advice during the study. A.C. provided advice and contributed to the WRF EURO-CORDEX simulations production and analysis. A.S. provided the initial version of the phenology modelling approach. All authors contributed to the article writing.

Methods

Pollen count observations. To calibrate and evaluate the models, we used observations of annual pollen counts over 51 sites across parts of Europe. Data are provided by the European Aeroallergen Network, which gathers observations from several national networks in Europe, the French aerobiology network RNSA (<http://www.pollens.fr>), the ARPA-Veneto, Italy (<http://www.arpa.veneto.it>), and from Croatian organizations, including the Institute of Public Health (counties of Brodsko-Posavska and Splitsko-Dalmatinska), the Department of Environmental Protection, Health Ecology Institute of Public Health 'Andrija Stampar' (Zagreb) and Associate-degree college of Velika Gorica.

Current ragweed density distribution. Ragweed density distribution was estimated using an observation-based database of ragweed presence (cells of 10×10 km; ref. 5). Distinction was made between countries which are estimated of sufficient quality⁵ (see their Figure 3.33) and other countries. In the first case, a prior distribution within each model grid cell is calculated as:

$$D_p(x, y) = I(x, y)LU(x, y)CI(x, y) \left(\frac{K(x, y)}{25} \right)^2$$

$I(x, y)$ describes the maximal density of ragweed plants per m^2 that would be obtained in the most suitable habitats. $LU(x, y)$ is the surface fraction of suitable land use, here taken as the crop and urban lands, and using the CMIP5 land-use classification for 2005 (ref. 29), which scales the surface of suitable habitats in the grid cell. $CI(x, y)$ is a climate index describing climate suitability for ragweed³. $K(x, y)$ is the number of 10×10 km cells with ragweed presence in the 50 km model grid cell. $(K(x, y)/25)^2$ is taken as an infestation factor describing the fraction of suitable land that is actually infested. See Supplementary Information for further details. For countries with low-quality presence inventories, or for countries where ragweed observations were not reported, we approximate the infestation factor by the average over countries with reliable data. To account for the proximity of neighbouring countries, we used a weighted average, which is proportional to the cube of the inverse of the distance of the grid cells. The density distribution was then calibrated for the simulated concentrations for the past years to fit mean annual observed counts (see Supplementary Information).

Weather and climate. Weather variables are taken from the regional climate models (RCMs) WRF and RegCM simulations over a large European domain, driven at the boundaries by global re-analyses (ERA-Interim) for model calibration and evaluation (hindcasts), and global coupled models (GCMs) for climate impact simulations. The IPSL-CM5A-MR/WRF (EURO-CORDEX low-resolution simulations; refs 19,30) and HadGEM/RegCM were used.

Pollen production. To calculate the pollen production, it was assumed that total pollen production is proportional to the biomass during the growing season using the formulation of Fumanal *et al.*³¹ expressed as:

$$\log_{10}(\text{total grain production}) = 7.22 + 1.12 \log_{10}(\text{plant biomass})$$

This formulation is implemented in the ORCHIDEE (ref. 17) land-surface model, which simulates the response of plant productivity to various environmental conditions, including climate variables and atmospheric CO_2 . Standard 'C3 grassland' plant functional type has been adapted to specifically represent the ragweed plant. We assume that total pollen production is distributed over the pollen production period by a bell-shape function. To determine the dates of start and end of the pollen season, we developed a process-based phenological model for ragweed using the Phenology Modelling Platform¹⁶, which takes into account two phases for ragweed development: germination (depending on 2 m air temperature and soil moisture) and growth (depending on 2 m air temperature and photoperiod)—see Supplementary Information for more details. Using data on estimated dates of the beginning and the end of pollen season from a set of pollen count stations, the PMP parameters are fitted and then used in ORCHIDEE to

predict ragweed phenology. The observed start and end dates of season are calculated as the days achieving respectively 1% and 99% of the year sum taken between 1 July and 15 October of each year.

Pollen release. We adapted the formulation in ref. 12 for the pollen flux (F) per plant (in grain $m^{-2} s^{-1}$),

$$F = aK_c \frac{P}{LAI \cdot H} u_*$$

where K_c is a time-varying factor depending on weather, u_* is the friction velocity, P is the daily production by the canopy per m^2 (calculated by ORCHIDEE as above), $LAI = 3$ is the leaf area index, $H = 1$ m is a canopy height and $a = 5 \times 10^{-4}$ day is a constant taken to correspond to that of the formulation in ref. 12. The main adaptation here was to consider a variable yearly production depending on weather, as calculated from the ORCHIDEE model, instead of a constant annual production.

Pollen dispersion. The dispersion is calculated from the CHIMERE (ref. 18) and RegCM (ref. 21) models. In CHIMERE, pollen grains are treated as aerosols. The mean diameter of the pollen grains corresponds to the largest bin in the model aerosol size distribution, between 10 and 20 μm . The effective diameter used in the gravitational settling parameterization is thus approximately 15 μm , which falls at the low end of the range of values usually used. The pollen density is 1,200 $kg m^{-3}$. The gravitational settling, with typical velocity of 1 $cm s^{-1}$, is the main dry deposition process for pollens and the only one considered in the model. The simulated pollen grains are transported by the atmospheric circulation and turbulent mixing, settled under the gravity, and washed out by in- and below-cloud scavenging, following the parameterizations already implemented for other CHIMERE aerosols. In RegCM, once emitted (see Pollen release), pollen particles are treated like a monodisperse aerosol of 20 μm diameter with a density of 1,200 $kg m^{-3}$. They undergo processes of advection, turbulent diffusion, convective transport, gravitational settling, dry deposition and washout. The uncertainty range on ragweed pollen diameter is roughly covered by the use of two values in this study.

Future ragweed distribution. A simplified approach of plant invasion accounting for habitat suitability in the changing climate and land use has been used. Starting from the current calibrated distributions, we assumed that the distribution at year n results from a progressive dispersal of seeds with a flux between two model grid cells inversely proportional to their square distance. The establishment of new plants from the seed flux then depends on target cell habitat suitability and its degree of already present infestation. See Supplementary Information for more details.

Numerical experiments. We performed three types of simulations—hind-cast, historical and future simulations—using two RCTM CHIMERE and REGCM. The hindcast simulations (HC) are performed to best simulate the pollen concentrations over a 13-year observation period (2000–2012) forced by ERA-Interim reanalysis. The historical simulations (HIST) are carried out for 20-year period (1986–2005) driven by a global climate model (GCM) and using calibrated ragweed density to serve as a reference simulation for the future.

References

29. Hurtt, G. C. *et al.* The underpinnings of land-use history: Three centuries of global gridded land-use transitions, wood harvest activity, and resulting secondary lands. *Glob. Change Biol.* **12**, 1208–1229 (2006).
30. Jacob, *et al.* EURO-CORDEX: New high-resolution climate change projections for European impact research. *Reg. Environ. Change* **14**, 563–578 (2014).
31. Fumanal, B., Chauvel, B. & Bretagnolle, F. Estimation of pollen and seed production of common ragweed in France. *Ann. Agric. Environ. Med.* **14**, 233–236 (2007).